The role of nanocrystalline cellulose on the microstructure of foamed castor-oil polyurethane nanocomposites

Andrés Ignacio Cordero[a], Javier Ignacio Amalvy[a], Elena Fortunati[b], José María Kenny[b], Leonel Matías Chiacchiarelli[c,*]

[a] Instituto de Investigaciones Fisicoquímicas Teóricas y Aplicadas (INIFTA), CCT La Plata CONICET-UNLP, Diag. 113 y 64, La Plata, Argentina
[b] Materials Engineering Center, UdR INSTM, University of Perugia, Strada di Pentima 4 05100 Terni, Italy
[c] Instituto de Tecnología de Polímeros y Nanotecnología (ITPN), CONICET-UBA, Buenos Aires, Argentina

Keywords:
Polyurethane foams
Castor oil polyol
Nanocrystalline cellulose
Mechanical properties
Thermal properties

A B S T R A C T

Nanocrystalline cellulose (CNC), obtained by sulphuric acid hydrolysis, was used to synthesize polyurethane foams (PUFs) based on a functionalized castor oil polyol and a Methylene diphenyl diisocyanate (MDI). Formulations with varying isocyanate index (FI) and NCO number were prepared. At 0.5 wt.%, SEM's of the fractured surface underlined that the CNC acted both as a nucleation agent and as a particulate surfactant with cell geometries and apparent density changing selectively. The chemical structure of the PUF (FTIR) changed after the incorporation of CNC by a relative change of the amount of urea, urethane and isocyanurate groups. A low NCO number and isocyanate index contributed to the migration of the CNC to the Hard Segment (HS), acting as reinforcement and improving substantially the compressive mechanical properties (E_c and σ_c improvements of 63 and 50%, respectively). For a high NCO number or isocyanate index, the CNC migrated to the Soft Segment (SS), without causing a reinforcement effect. The migration of the CNC was also detected with DSC, TGA and DMA, furtherly supporting the hypothesis that a low NCO number and index contributed both to the formation of a microstructure with a higher content of urethane groups.

1. Introduction

Polyurethane foams (PUFs) represent a relevant class of materials with several industrial applications, ranging from insulation panels, structural reinforcement, sandwich construction to medical applications (Randall & Lee, 2003; Szycher, 1999). Due to the elevated worldwide production of those foams and the fact that most of its precursors are obtained from non-renewable resources, it becomes of utmost importance to develop foam precursors which are obtained from renewable resources, such as biomass. Traditional PUF formulations are composed of a polyol, an isocyanate and several additives. The chemical reaction of those precursors leads to a complex structure, which can be composed of interpenetrated molecules with different molecular weights, functionalization and cristallinity. A simplified picture of the microstructure of PUF can be visualized as a void structure interpenetrated with a solid polyurethane polymer. The solid polyurethane can also be understood as being composed of Soft (SS) and Hard Segments (HS), which are obtained from the polyol and isocyanate precursors, respectively. The distribution of the SS and HS and its physical and chemical properties determine the final properties of the solid part of the PUF. In addition, a typical PUF is composed of HS which have a distinct chemical structure, with urethane, urea and isocyanurate groups usually present. In addition, the molecular arrangement and the hydrogen type interaction among chains represent a key determinant aspect with respect to the final mechanical and thermal properties (Petrović, Cho, Javni, Magonov, &, Yerina, 2004; Tien & Wei, 2001). As far as the void content is concerned, i.e., what its known as foams cells, the most important aspects are related to its geometry, volumetric concentration, wall type (closed or open cell) and inert gas content. Those characteristics determine the mechanical, thermal and insulation properties of the resulting foam.

The precursors of PUFs which are frequently used industrially are mostly synthesized from non-renewable resources, i.e., petrochemical derivatives. However, over the last decades, several researchers have studied the incorporation of vegetable oils into the formulation of foamed polyurethanes. Particularly, due to the chemical structure of some vegetable oils, such as castor, soy-bean and others, it was plausible to replace the polyol component (obtained from non-renewable resources) with those without

* Corresponding author.
E-mail address: lmchiacchiarelli@yahoo.com.ar (L.M. Chiacchiarelli).

http://dx.doi.org/10.1016/j.carbpol.2015.07.077

the need of additional complex chemical reactions (Aranguren, Marcovich, Salgueiro, & Somoza, 2013; Aranguren, Rácz, & Marcovich, 2007; Casado, Marcovich, Aranguren, & Mosiewicki, 2009; Corcuera et al., 2010; Chen, Wang, & Wang, 2011; Hojabri, Kong, & Narine, 2009; Javni, Petrovic, Guo, & Fuller, 2000; Lin et al., 2013; Mosiewicki, Casado, Marcovich & Aranguren, 2009; Mosiewicki, Dell'Arciprete, Aranguren & Marcovich, 2009; Tamami, Sohn, & Wilkes, 2004; Wik, Aranguren, & Mosiewicki, 2011). It should be noticed that research related to the replacement of the polyol component obtained from petrochemical derivatives with non-renewable counterparts has been the main research area so as to develop bio-based PUF. However, the isocyanate component represents a substantial weight fraction of the PUF formulation. Nevertheless, it is generally accepted that research related to the obtention of isocyanate precursors from renewable resources has not led to an industrially viable path (Besse et al., 2013; Çaylı & Küsefoğlu, 2008). Then, taking into account that rigid foams are composed of a substantial weight fraction of HS, it can be inferred that the formulations will indeed contain a higher weight fraction of isocyanate and, hence, a lower content of components derived from renewable resources. To avoid this drawback, one option is to incorporate nanoparticles into the formulation which can replace the HS obtained from the isocyanate precursor. Then, if the nanoparticle is obtained from renewable resources, formulations with a higher content of renewable precursors could be synthesized. Several nanoparticles are available to that purpose, however, one of the most relevant nanostructures which has been intensively studied over the last years is nanocrystalline cellulose (Alvarez & Vázquez, 2004; Brinchi, Cotana, Fortunati, & Kenny, 2013; Klemm, Heublein, Fink, & Bohn, 2005; Alvarez, Cyras, & Vázquez, 2008). Its main features are that it is an abundant biopolymer, with industrial productions of approximately 10^{12} tons a year and it is renewable and biodegradable in nature (Klemm, Schmauder, & Heinze, 2005). In addition, the nanometric geometry of the CNC confers outstanding mechanical properties, with an elastic modulus which is similar or greater than Kevlar and tensile strengths in the order of 10^3 MPa or more. However, to fully exploit its properties, the CNC must be incorporated as reinforcement in a nanocomposite. This subject has been extensively studied by several researchers (Aranguren et al., 2013; Auad, Contos, Nutt, Aranguren, & Marcovich, 2008 Casado et al., 2009; Juntaro, Ummartyotin, Sain, & Manuspiya, 2012; Özgür Seydibeyoğlu and Oksman, 2008; Rueda et al., 2013; Wik et al., 2011). On the other hand, for the particular case of a PUF matrix, only few studies have been published so far. The group of Li et al. (Li & Ragauskas, 2011, 2012; Li, Ren, & Ragauskas, 2010, 2011) has studied the development of bio-based PUF reinforced with CNC added at a concentration ranged from 0.2 up to 5 wt.%. Using FTIR, the authors found that the CNC was hydrogen bonded with the HS and it was asserted that the addition of CNC increased the phase separation of the SS and the HS. The cell diameters decreased as a function of increasing content of CNC but the density followed a non-monotonous change as a function of CNC content. The CNC was also believed to act as a nucleation agent. It was asserted that the dominant chemical structure of the foam did not change with the addition of CNC. Finally, the addition of CNC dramatically improved the mechanical properties of the resulting foams. Another group, led by Mosiewicki, Rojek, Michałowski, Aranguren, and Prociak (2015), have studied the incorporation of cellulose micro-nanocrystals (MNC) in a rapeseed-oil based PUF. Its incorporation did not significantly modify the apparent density, the thermal conductivity and the closed cell of the foam. However, a significant increase of water absorption was measured as a function of increasing MNC content. In addition, dynamical thermo-mechanical and compression tests were performed, obtaining an increase in the glass transition temperature and compressive rigidity. Other works have attempted the incorporation of cellulose into PU, however, the materials developed fall into the classification of composites rather than nanocomposites (Mosiewicki, Dell'Arciprete, Aranguren & Marcovich, 2009; Rivera-Armenta, Heinze, & Mendoza-Martínez, 2004; Silva, Takahashi, Chaussy, Belgacem, & Silva, 2010; Wik et al., 2011).

In this work, the effect of the incorporation of the CNC in a PUF was evaluated using several characterization techniques. The most significant variables under analysis were the isocyanate formulation index (FI), the isocyanate number and the CNC content while the most significant properties measured were the apparent density, cell size, anisotropy factor, compressive mechanical properties, storage modulus and damping factor (DMA), thermal transitions (DSC), weight residue (TGA) and chemical structure (FTIR).

2. Materials & methods

Castor Oil (Parafarm 99.9%, P_{157}) was used as the polyol, with an hydroxyl value of 157 mg KOH mg^{-1} determined by acetylation with acetic anhydride in pyridine solution, according to the ASTM D4274-99 (Test Method A). Glycerol (99.9%), which was used as a crosslinker, was purchased from Research AG. Methylene diphenyl diisocyanate (MDI), commercially known as Suprasec 9584 (ISO_1) and 5005 (ISO_2), were used. The first one had a functionality of 2.67 and a NCO number of 24.1%, while the second one 2.66 and 31.0% respectively. Before any sample was synthesized, NCO numbers were determined using the procedure of the ASTM D2572 standard. A silicone based surfactant, denominated Niax L-585, was also used in the formulation (supplied by Resikem). Dibutyltin dilaurate (DBTDL, 95%) was used as the catalyst and it was kindly supplied by Mentvil Argentina. Distilled water (18.2 MΩ) was used as the blowing agent. Microcrystalline cellulose (MCC, dimensions of 10–15 μm), supplied by Sigma–Aldrich, was used as precursor to extract nanocrystalline cellulose with nanometric dimensions (CNC). To achieve this, MCC was hydrolyzed with sulphuric acid (64 wt.%) at 45 °C for 30 min, following what has been done in previous works (Cranston & Gray, 2006; Fortunati et al., 2012b). A centrifugation and a dialysis procedure were applied in order to remove the acid excess while a mixed bed ion exchange resin (Dowex Marathon MR-3 hydrogen and hydroxide form) was added to the cellulose suspension for 48 h and then removed by filtration (traces of Ca and Si could migrate to the CNC during dialysis). The resultant nanocrystalline cellulose aqueous suspension was sonicated (Vibracell 750) for 5 min. in an ice-bath. Additionally, the CNC was thermally neutralized by addition of 1.0 vol.% of 0.25 M NaOH. The final CNCs water suspension had approximately 0.5 wt.% of CNC, with a calculated hydrolysis yield of approximately 20%. The obtained CNC showed the typical acicular structure with dimensions ranging from 100 to 200 nm in length and 5–10 nm in width, as previously reported in other works of the group (Fortunati et al., 2012a,b). A TEM image of the CNC used in this work has been reproduced by other works of the authors (Fig. 1).

A typical formulation for a semi-rigid PUF was used. Formulations with two isocyanate indexes of 105 and 115 were prepared. The foams obtained with indexes 105 and 115 will be denominated FX_1 and FX_2, respectively, where X stands for the specific formulation (Table 1).

Formulations prepared with F1 and F2 were obtained from isocyanates with a higher NCO content. Hence, the specific weight fraction of HS will decrease from F1 to F2, respectively. The preparation of the PUF was based on the one-shot method (Randall & Lee, 2003). For each formulation, at least two preparations were made, so as to corroborate the reproducibility of the results. For the case of PUF prepared with CNC, a concentration of 0.5 wt.% of CNC was fixed for all the work presented in this manuscript. It was initially

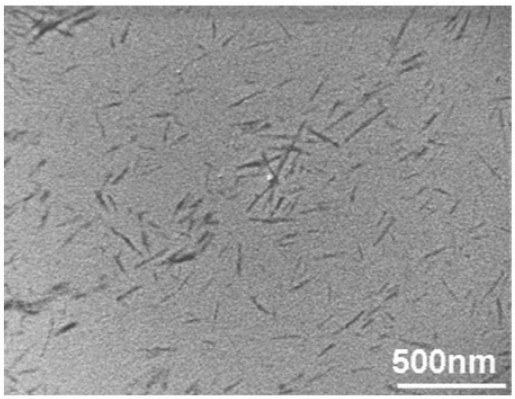

Fig. 1. Reprinted from Fortunati et al. (2015a).

Table 1
PUFs formulations.

Formulations /component	$F1_1$	$F1_2$	F2
ISO_1	185	207	–
ISO_2	–	–	147
P_{157}	100	100	100
Glycerol	20	20	20
Blowing agent	1	1	1
Catalyst	1	1	1
Surfactant	5	5	5
FI	105	115	105

dispersed in the polyol after applying a combined sonication and homogenization dispersion procedure, which was used in previous works of the author (Chiacchiarelli, Monsalve, Vazquez, Kenny, & Torre, 2014; Chiacchiarelli, Escobar, Kenny, Torre, & Vazquez, 2015). It consisted of a total amount of 300 min. of sonication (Tegostab T60) and 15 min. of homogenization, separated in 5 min. steps to avoid a substantial increase of polyol temperature. Post-cure of each PUF was done at 120 °C for one hour. To corroborate that the PUF samples did not have any isocyanate group unreacted, FTIR absorption spectra was utilized to confirm that no absorption centered at 2270 cm^{-1} was present. FTIR absorption spectra were obtained with a Shimadzu IRAffinity using the Attenuated Total Reflection (ATR) methodology (ZnSe prism with and incidence angle of 45°). It is important to notice that the dimensions of the prism were approximately 10 mm by 10 cm, hence, for each measurement, a wide sample area was covered. Each spectrum was obtained from 60 scans at a resolution of 4.0 cm^{-1} and corrected for ATR. As far as the quantitative analysis is concerned, the FTIR absorption centered at 1595 cm^{-1}, which can be associated to the absorption of a phenyl group, was used to normalize each spectrum. Even though in literature (Tien & Wei, 2001) it is frequent to use the C-H absorbance centered at 2935 cm^{-1}, we have chosen the methodology implemented by Modesti and Lorenzetti (2001), because it is suitable for the PUF studied in this work.

Apparent density was measured by cutting squares of 1 cm sides and by measuring its weight. Compressive mechanical analysis was performed with an Instron 5985 universal testing machine, following the guidelines of the standard ASTM D1621. At least 10 samples were tested for each formulation. Thermogravimetric (TGA) analysis was performed using Shimadzu TGA 50 under a nitrogen atmosphere. The thermal experiment started at room temperature and went up to 800 °C at a constant rate of 10 °C min^{-1}. At least three samples were tested for each formulation studied. Differential Scanning Calorimetry (DSC) was performed with a TA instruments Q200 where its calibration was performed automatically and periodically by means of an internal standard. At least three samples of each formulation were tested. To obtain the thermal transitions of the formulations, a full thermal cycle was implemented, which consisted of three thermal cycles. The first one started at −80 °C and went up to 200 °C at a scan rate of 10 °C min^{-1}. The second one started at 200 °C and went down to −80 °C at 15 °C min^{-1} and, finally, the third one was identical to the first cycle. Dynamic Mechanical Analysis was carried out with a Perkin & Elmer DMA 8000. The simple cantilever bending mode was used, fixing the oscillation frequency to 1.0 Hz and the amplitude to 0.05 Hz. The thermal scan started at 0 °C and went up to 180 °C at a scan rate of 2 °C min^{-1}. Experiments as a function of deformation (amplitude) were carried out in order to corroborate that the deformation fell into the linear viscoelastic region of the material. At least three samples were tested for each formulation.

3. Results and discussion

3.1. Apparent density of the PUFs

The average apparent densities (ρ_{AVG}) of the studied foams are reported on Table 2. Due to the fact that the ρ_{AVG} of all the PUFs studied were in the range 139–220 kg m^{-3}, it can be deduced that semi-rigid and rigid foams were developed in this work.

As far as the foam $F1_1$ is concerned, a ρ_{AVG} of $1 \times 79.10^2 \pm 7.93$ was measured, which was also similar to the $F1_2$. In addition, it is important to notice that its statistical dispersion was small. Then, the foam growth resulted on a density which was roughly independent of the FI. This result was expected because a higher index should not alter the growth stage significantly so as to observe a substantial variation of ρ_{AVG}. On the other hand, comparing the PUFs prepared with $F1_1$ and F2, it can be inferred that the increase of the NCO number caused a significant decrease of the ρ_{AVG}, a result to be expected due to the faster crosslinking kinetics of the formulation. In contrast, the addition of CNC into the formulation changed substantially the ρ_{AVG} only for the case of $F1_1$. The incorporation of 0.5 wt.% of CNC increased the ρ_{AVG} by approximately 20%. In addition, the statistical dispersion was also significantly increased, by approximately 40%. Then, it can be concluded that the addition of CNC changed considerably the growth stage, producing denser PUF but, more importantly, a PUF with a more heterogeneous microstructure. However, on the other formulations, the ρ_{AVG} did not change substantially with the addition of CNC but, instead, only changed its heterogeneity. Comparing these results with what has been found in literature, Mosiewicki et al. (2015) found that the addition of nanometric cellulose (up to 3 wt.%) did not significantly modify the apparent density, while Li and Ragauskas (2012) and Li et al. (2010, 2011) found that the addition of nanometric cellulose (up to 5 wt.%) did not have a monotonous increase, instead, it decreased up to a CNC concentration of 0.75 wt.% and increased afterwards (using pentane as a blowing agent). Then, our work follows what has been found by the second group of researchers, in other words, that the addition of CNC might increase or decrease the apparent density of the PUF but to an extent dependent on its specific formulation. It is important to notice that the hypothesis used to explain the measured change of apparent density was related to the fact that the CNC would act as a nucleation agent during the growth stage. However, the sole measurement of apparent density should not be used as a conclusive fact of that relationship. In our work, based only on the indirect ρ_{AVG} measure, it can be inferred that the CNC served as a nucleation agent only for the case of the $F1_1$ formulation. In the following section, cell size and heterogeneity will also be taken into account so as to obtain a more substantiated conclusion about the nucleation effect of CNCs in the PUFs.

Table 2
Geometrical and mechanical properties of the PUF samples.

Formulations	ρ_{AVG} (kg m^{-3})	Cell Size (um)	Anisotropy Factor	E_c(MPa)	σ_c (MPa)
$F1_1$	$1.79 \times 10^2 \pm 7.93$	L: $2.02 \times 10^{2 \pm 47.1}$ T: $1.38 \times 10^{2 \pm 30.2}$	1.46	$3.86 \times 10^1 \pm 13.3$	1.44 ± 0.14
$F1_1$-0.5 wt.% CNC	$2.14 \times 10^2 \pm 10.9$	L: $2.66 \times 102^{\pm 72.0}$ T: $1.68 \times 10^{\pm 40.0}$	1.58	$6.30 \times 10^1 \pm 14.0$	2.16 ± 0.22
$F1_2$	$1.75 \times 10^2 \pm 4.99$	L: $3.06 \times 10^{2 \pm 75.0}$ T: $1.82 \times 10^{2 \pm 33.9}$	1.68	$6.13 \times 10^1 \pm 14.2$	1.54 ± 0.24
$F1_2$-0.5 wt.% CNC	$1.81 \times 10^2 \pm 25.0$	L: $2.02 \times 10^{2 \pm 43.8}$ T: $1.42 \times 10^{2 \pm 31.9}$	1.42	$2.07 \times 10^1 \pm 5.3$	1.07 ± 0.13
F2	$1.39 \times 10^2 \pm 11.0$	L: $3.29 \times 10^{2 \pm 87.0}$ T: $1.59 \times 10^{2 \pm 47.5}$	2.07	$4.74 \times 10^1 \pm 9.76$	1.28 ± 0.22
F2-0.5 wt.% CNC	$1.34 \times 10^2 \pm 11.3$	L: $1.82 \times 10^{2 \pm 54.4}$ T: $2.25 \times 10^{2 \pm 78.8}$	8.1×10^{-1}	$4.30 \times 10^1 \pm 14.3$	1.22 ± 0.32

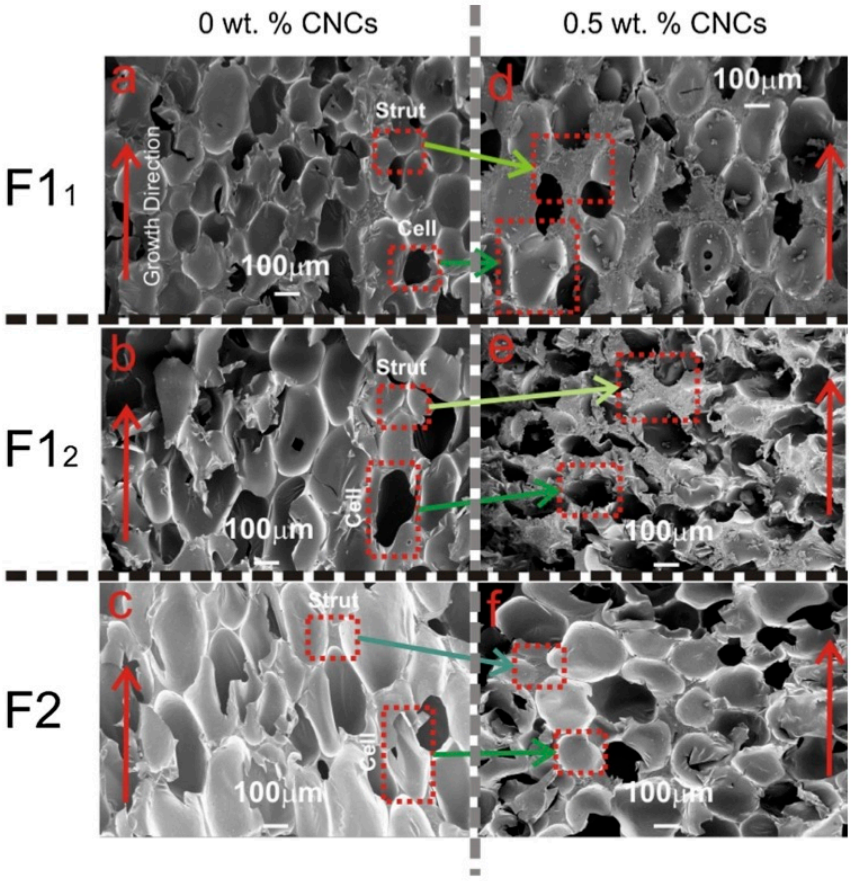

Fig. 2. SEM fractured surface of the following PUFs: a) $F1_1$, b) $F1_2$, c) F2, d) $F1_1$-0.5 wt.% CNC, e) $F1_2$-0.5 wt.% CNC and f) F2-0.5 wt.% CNC. Growth direction marked with an arrow.

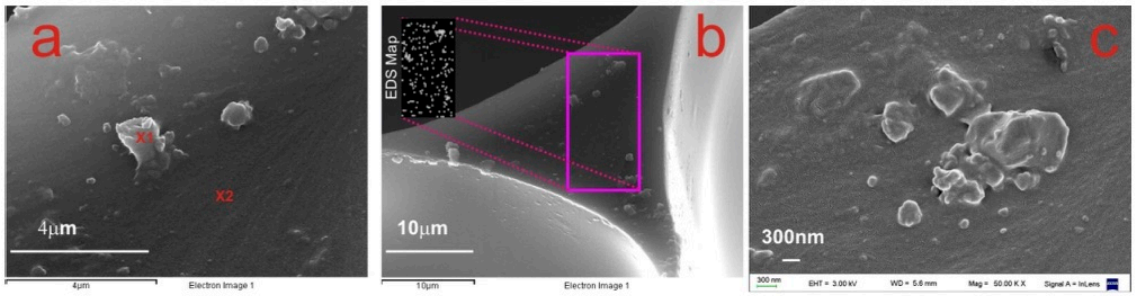

Fig. 3. EDS analysis of the PUF reinforced with CNC. a) Punctual compositional evaluation b) mapped compositional analysis for Ca c) Magnification of the agglomerate shown in part a.

3.2. Fractured surface analysis

The fractured surface of the PUF prepared with $F1_1$ is shown in Fig. 2a. On the left column, the fractured surfaces of the formulations $F1_1$, $F1_2$ and F2 are depicted. On the right column, the fractured surfaces of identical formulations but prepared with 0.5 wt.% CNC are also depicted. The vertical red arrows within each graph represent the PUF growth direction.

The features that can be distinguished at this magnification (200×) were the size and geometry of the cell windows and how each cell intersected others, forming the cell struts (all these features are highlighted with red boxes within each graph). The statistical analysis of the cell dimensions and apparent density is reported on Table 2.This included the cell dimension on the direction parallel (L) and perpendicular (T) to the growth direction as well as the anisotropy factor (AF), which was defined as the ratio of the dimension parallel to the growth direction to the perpendicular one. All these measurements can be used to deduce if the CNC behaved or not as a nucleation agent, providing a complementary measurement to the apparent density results presented in Section 3.1.

As far as the PUF prepared from $F1_1$, it is cell was anisotropic, having a larger dimension parallel to the growth direction, an expected result because its molded nature .With respect to the cell size, an average value of 202 μm (L) was found. On the other side, the fractured surface of the PUF prepared with $F1_2$ is depicted in Fig. 2b. The difference between $F1_1$ and $F1_2$ was the FI. Then, it can be inferred that the foam prepared with $F1_2$ had cells with bigger dimensions, both in the L and T directions. In contrast, the apparent density of both foams was found to be similar. Hence, it is logical to assume that the amount of cells in the foam prepared with $F1_2$ was smaller with respect to the foam prepared with $F1_1$. Taking into account that the $F1_1$ had a reduced FI with respect to the $F1_2$, it can be concluded that an increased index caused a change of the cell size but an overall null change of the apparent density of the foam, a conclusion that was also obtained from the ρ_{AVG} values discussed in Section 3.1. Finally, the PUF prepared with F2 is depicted in Fig. 2c. Due to the fact that the difference among $F1_1$ and F2 was the NCO number, it can be inferred that a higher NCO number formed a PUF with bigger cell dimensions, both in the L and T directions. In addition, as it was mentioned in Section 3.1, its apparent density decreased. These experimental results were expected because an increase of the NCO number would produce a formulation with a lower weight content of the isocyanate precursor. This, in turn, would imply a higher concentration of the blowing agent, producing a PUF with a reduced apparent density.

As far as the PUF prepared with CNC is concerned, the fractured surfaces of the PUFs prepared with $F1_1$-0.5 wt.% CNC, $F1_2$-0.5 wt.% CNC and F2-0.5 wt.% CNC are depicted in Fig. 2c and d, and Fig1e, respectively. Comparing the micrographs with the PUFs prepared with $F1_1$, $F1_2$ and F2 (left column in Fig. 1), it can be concluded that significant changes of the fractured surface were found. This indicated that the CNC had a substantial role in both the formation of the cell windows and struts and its subsequent rupture in all the studied formulations. The most relevant aspects observed were that the struts had, in general, increased dimensions (coarser nature) and that the CNC distribution was also concentrated on the struts, leaving cell windows with, probably, a different concentration of CNC. As far as the cell size is concerned (Table 2), the CNC had an effect that depended on both the FI and the NCO number. Specifically, the cell dimensions increased for the case of PUF reinforced with CNC and prepared only with $F1_1$. In contrast, for the other two formulations, $F1_2$ and F2, the opposite effect was measured.

The previous experimental observations can be used to deduce the role of CNC as a nucleation agent and a particulate surfactant. For the particular case of $F1_1$, the results indicated that the CNC behaved mostly as a particulate surfactant. This effect can be inferred from the coarser nature of the struts (Fig1a and d). Hence, during PUF growth, the CNC retarded the cell window drainage rate forming a coarser cell structure (Fig. 2d). Also, because of the results presented in Section 3.1, it can be inferred that the indirect apparent density measurement could lead to non substantiated conclusion, i.e., to deduce that the CNC behaved as a nucleation agent. On the other hand, for the case of PUF prepared with formulations $F1_2$ and F2, the incorporation of CNC into the formulation indicated that, during foam growth, it behaved both as a nucleation agent and a particulate surfactant. As far as the nucleation effect is concerned, in both cases the incorporation of CNC reduced substantially the cell dimensions in both the L and T directions. On the other hand, the CNC also behaved as a particulate surfactant, a fact that can also be assumed from the coarser nature of the struts. As well as in the other formulations, the CNC increased the surface tension, counteracting the effect of the Niax-L585 surfactant.

Then, it can be concluded that the change of the FI or the NCO number in the PUF formulation altered the role of CNC during PUF growth. Specifically, when the formulation had a lower NCO number and a reduced FI, it implied that the CNC would only behave as a particulate surfactant. On the other hand, after changing either the NCO number or the FI in the formulation, it was found that the CNC behaved both as a nucleation agent and a particulate surfactant.

As far as the dispersion of the CNC in the PUF is concerned, Energy Dispersive X-Ray Spectroscopy (EDS) was used to determine the CNC distribution within the PUF matrix. Due the fact that the CNC had a nanometric geometry and the PUF matrix had an interpenetrated network morphology (also with nanometric features), it was important to analyze the dispersion with an alternative technique. To this effect, EDS compositional maps of the PUFs were determined, as depicted in Fig. 3. A compositional EDS analysis of an CNCs agglomerate (Fig. 3a, denoted as X1) presented the following composition: C_K: 49.10 wt.%; O_K: 35.51 wt.%; Si_K: 3.19 wt.%; S_K: 0.83 wt.% and Ca_K: 11.38 wt.%. In contrast, the bulk PUF (Fig. 3a, denoted as X2), presented the following composition: C_K: 82.57 wt.%; O_K: 15.35 wt.%; Si_K: 2.08 wt.%. Then, it can be inferred that Ca and S (to a lesser extent) can be used to identify the distribution of the CNCs in the PUF matrix. To further corroborate that the agglomerate shown in Fig. 2a corresponded to a CNC agglomerate, a magnified micrograph is shown in Fig. 2c. Finally, a compositional map of Ca for a strut of a PUF reinforced with CNCs is depicted in Fig. 3b.

3.3. Infrared absorption spectra of the PUFs

The infrared absorption spectra of the PUF samples prepared from the formulations reported in Table 1 is shown in Fig. 4. The spectra presented several infrared absorptions associated to the microstructure of the PUF, which can be found elsewhere (Lee, Wang, & Hsu, 1987). The absorptions studied in this work were the phenyl (1595 cm^{-1}), urethane (1220 cm^{-1}), isocyanurate (1413 cm^{-1}) and urea (1510 cm^{-1}) groups. In addition, the infrared absorptions due to the free and H bonded —NH stretching modes, 3480 cm^{-1} and 3320 cm^{-1}, respectively, were also used in the analysis. It is important to notice that the phenyl group was used for normalization purposes.

In literature, it is frequent to use the C—H absorption band centered at 2935 cm^{-1}, however, because the incorporation of CNC in the matrix prevents the use of that region (absorption overlapping), the methodology implemented by Modesti and Lorenzetti (2001) will be used instead. All the PUF prepared in this work did not have an absorption band centered at 2270 cm^{-1}, indicating that no free isocyanate groups were left unreacted. In order to develop an approximate composition of the PUFs, a quantification using the previous mentioned absorptions bands was performed, using the

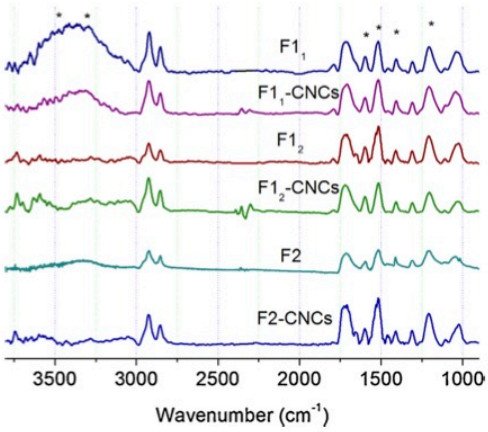

Fig. 4. FTIR absorption spectra of the PUF samples.

Table 3
FTIR quantification of the PUF formulations.

Formulation	$A_{Urethane}$	$A_{Isocyanurate}$	A_{Urea}
$F1_1$	4.77 ± 0.15	1.29±0.05	4.42 ± 0.21
$F1_1$ - 0.5 wt.% CNCs	5.97 ± 0.20	1.05±0.17	4.57 ± 0.19
$F1_2$	4.73 ± 0.05	8.84×10^{-1} ±0.03	4.32 ± 0.33
$F1_2$-0.5 wt.% CNCs	2.71 ± 0.13	6.62×10^{-1} ±0.02	2.69 ± 0.41
F2	4.78 ± 0.10	6.48×10^{-1} ±0.1	3.51 ± 0.11
F2-0.5 wt.% CNCs	4.19 ± 0.14	5.78×10^{-1} ±0.09	3.82 ± 0.29

area of the absorption band of the phenyl group to normalize the results. The results of this analysis are reported on Table 3, where the effect of changing the FI, the incorporation of CNCs and the modification of the NCO number are reported. The most significant aspect which can be inferred from Table 3 is that the incorporation of CNC in the formulation changed the content and distribution of urethane, isocyanurate and urea groups and this effect was consistently measured for all formulations.

It is important to contrast these experimental results with what has been found in literature (Faruk, Sain, Farnood, Pan, & Xiao, 2014; Li et al., 2010, 2011; Mosiewicki et al., 2015; Rivera-Armenta et al., 2004). Specifically, it was asserted that the addition of CNC did not change the chemical composition of the PUF. On the contrary, the authors of this work considered that the incorporation of CNC changed the nature and distribution of the chemical groups present on the microstructure of the PUF due to the hydroxides groups present on the surface of the CNC that probably react with the isocyanate precursor. Then, it can be assumed that the CNC was not only acting as a nucleation agent or particulate surfactant but that it also modified the urethane, urea and isocyanurate kinetics. Another aspect to notice is that the incorporation of CNC consistently decreased the relative amounts of urethane, isocyanurate and urea groups of all the formulations except for the $F1_1$. Hence, the hydroxide groups present on the surface of the CNC probably caused substantial hydrogen bonding in-between the SS, preventing the formation of additional urethane, isocyanurate and urea groups. In contrast, for the specific case of the $F1_1$, the absorption band centered at 3480 cm^{-1} indicated the presence of urethane groups with free hydrogen bonded N—H groups. Then, it can be inferred that for the particular case of $F1_1$, the isocyanate preferred to react with the hydroxide groups present on the anhydroglucose unit (AGU) of the CNC instead of forming compact hydrogen bonded HS. This hypothesis was confirmed because the addition of CNC in the $F1_1$ caused an increase of the urethane groups and a simultaneous decrease of the absorption band centered at 3480 cm^{-1}. Subsequent experimental sections will also corroborate this hypothesis.

3.4. Mechanical tests of the PUFs

The results of the compression tests, specifically the compressive elastic modulus (E_c) and strength (σ_c) are reported in Table 2. The results indicated that the change of the NCO number, the FI and the addition of CNC of the formulation altered both the E_c and the σ_c. Comparing the PUFs prepared with $F1_1$ and $F1_2$, then, an increased FI caused an improvement of both E_c (+58%) and σ_c (+6.9%), a result which was expected and logical. In addition, comparing the PUFs prepared with $F1_1$ and F2, then, a higher NCO number contributed to the formation of a PUF with similar σ_c but improved E_c (+22.8%). On the other hand, the incorporation of CNC on those formulations had an effect that depended on both the NCO number and the FI. For the PUF prepared with $F1_1$, the incorporation of CNC caused a substantial improvement of both E_c (+63%) and σ_c (+50%). For the $F1_2$, the incorporation of CNC caused a decrease of both E_c (−66%) and σ_c (−30.5%), while for the case of F2, the incorporation of CNC caused a decrease of E_c (−9.3%) and a similar σ_c.

The previous experimental results highlight that the role of the CNC in a PUF formulation can be associated to either a SS or a HS. For the case of formulation $F1_1$, the probable migration of the CNC to the HS implied that it reacted with the isocyanate precursor, forming additional urethane linkages (Section 3.3) and an improvement of its mechanical properties. This increase of mechanical properties would imply that the original formulation could be modified so as to reduce the total amount of HS. Assuming that the HS is obtained from the isocyanate precursor, a material with an increased content of precursors derived from renewable resources could be attained.

On the other hand, for the PUFs prepared with formulations $F1_2$ and F2, the CNC behaved as a SS, probably because the CNC did not migrate to the HS and it produced a detrimental effect on the mechanical properties. At first sight, this decrease of mechanical properties could be considered as a drawback. However, it is also relevant to emphasize that the CNC in those formulations could replace the SS, then, the PUF could be reformulated to contain a lesser amount of precursors which are derived from non-renewable resources (specially for applications where synthetic polyols are used).

3.5. Differential scanning calorimetry of the PUFs

The heat flow as a function of temperature of the PUFs showing the SS and HS thermal transitions is depicted in Figs. 5 and 6, , respectively. The location of the thermal transition of the SS is related to the glass transition temperature (Tg_{ss}) of the SS, as well as its HS counterpart (Tg_{HS}). As it can be inferred from Fig. 5, the location of the Tg_{ss} was selectively dependant on the FI, the NCO number and the presence of CNC. Specifically, a change of the FI (from Fig. 4a to c) and the NCO number (from Fig. 4a to e) had an irrelevant effect on the location of the Tg_{ss}. This behavior was expected because those variables would not alter the Tg_{ss}. On the other hand, the incorporation of CNC changed the location of the Tg_{ss} only for the formulations $F1_2$ (from Fig. 4c to d) and F2 (from Fig. 4e to f). In contrast, for the case of $F1_1$ (from Fig. 4a to b), the Tg_{ss} remained unaltered. Specifically, the Tg_{ss} increased by approximately 5 °C whenever the CNC was incorporated into the formulations $F1_2$ or F2 (it is important to notice that at least three repetitions were made to corroborate these results). This result was of paramount importance because it could be inferred that for the case of the $F1_2$ and F2 formulations, the CNC partially migrated to the SS microstructure, increasing the temperature where the Tg_{ss}

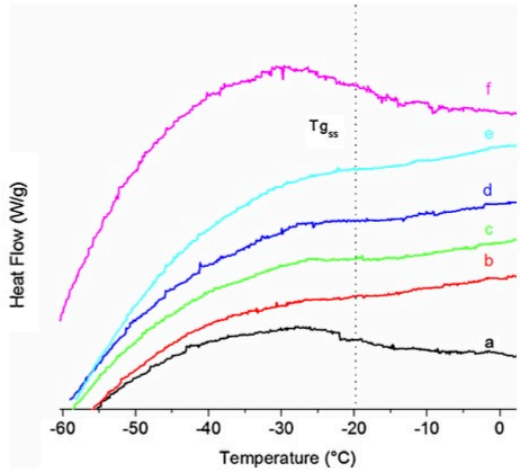

Fig. 5. Heat Flow as a function of temperature showing the SS transition of the PUFs samples, a) $F1_1$, b) $F1_1$-0.5 wt.% CNCs, c) $F1_2$, d) $F1_2$-0.5 wt.% CNCs, e) F2, f) F2-0.5 wt.% CNCs.

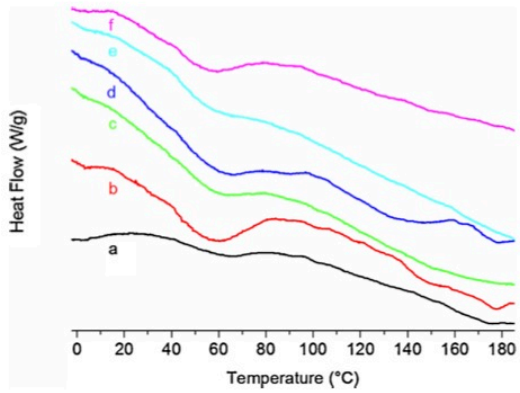

Fig. 6. Heat Flow as a function of temperature showing the HS transition of the PUFs samples, a) $F1_1$, b) $F1_1$-0.5 wt.% CNCs, c) $F1_2$, d) $F1_2$-0.5 wt.% CNCs, e) F2, f) F2-0.5 wt.% CNCs.

was centered. On the other hand, for the case of the $F1_1$ formulation, the CNC did not migrate to the SS microstructure because its Tg_{ss} remained unaltered. Due to the fact that the SS is responsible for the low temperature behavior of the PUF, it can be inferred that the CNC might improve its performance only for the case of the $F1_2$ and F2 formulations.

The heat flow as a function of temperature showing the HS transitions of the studied PUFs is depicted in Fig. 6.

For all formulations, transitions which covered a wide temperature range were found. The most relevant thermal transition, which was found on all formulations, covered a wide temperature range ($\Delta T \approx 30\,^{\circ}C$) and it was centered at approximately 40 °C (Tg_{HS1}) and it was associated to the formation of a urethane network. The existence of this transition was also corroborated with the DMA and FTIR results discussed in Sections 3.6 and 3.3, respectively. As it can be assumed, the location of the Tg_{HS1} was slightly dependant on the FI and the CNC but mostly dependant on the NCO number (from Fig. 5a to c). An increase of the former caused a higher Tg_{HS1}, which could be associated to a urethane HS with an improved hydrogen bonding interaction. On the other hand, the thermal transitions associated to the formation of isocyanurate or other networks (Tg_{HS2}) were found for temperatures above 80 °C.

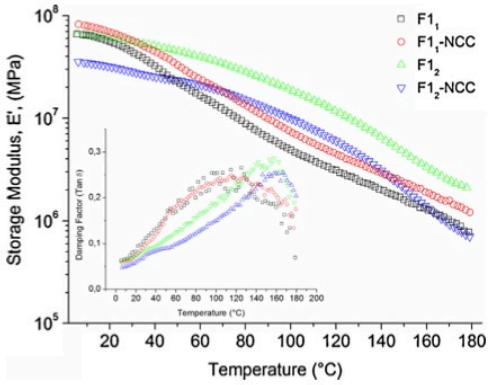

Fig. 7. Storage modulus (E') and damping factor (inset) versus temperature of the PUFs samples.

Even though small changes of the position and range of that transition were found as a function of the studied variables, no conclusive facts could be deduced from the experimental results.

3.6. Dynamic mechanical thermal analysis of the PUFs

The results of the DMA analysis of the PUFs prepared with $F1_1$ and $F1_2$ with and without CNC are shown in Fig. 7.

The main graphic corresponded to the storage modulus (E') as a function of temperature while the inset corresponded to the damping factor (tan δ) as a function of temperature. Comparing the E' of the PUF prepared with $F1_1$ and $F1_2$, it can be inferred that the E' of the $F1_2$ had an increased absolute value and it decreased less steeply as a function of temperature. In addition, from the damping factor graph it can also be assumed that the $F1_1$ and $F1_2$ had glass transition temperatures (T_g) centered at approximately 110 °C and 150 °C, respectively, as well as a common one centered at approximately 40 °C. Those thermal transitions can be related to the isocyanurate and urethane networks, as already discussed in Section 3.5. Because the $F1_2$ had an increased index with respect to the $F1_1$, these results were expected. On the other hand, the incorporation of the CNC had an effect which was dependent on the FI. For the case of the PUF prepared with $F1_1$, the incorporation of CNC in the formulation shifted the E' curve upwards while maintaining a similar damping factor plot. It is important to notice that these results are coherent with what has been found in other tests, such as the mechanical ones (Section 3.4). In addition, as already discussed in Section 3.1, the increased heterogeneity of the PUF prepared with CNC produced a plot with a higher scattering. For the case of the PUF prepared with $F1_2$, the incorporation of CNC in the formulation shifted the E' curve downwards, indicating a deterioration of the storage modulus of the PUF as a function of temperature. The damping factor also indicated that the T_g increased slightly and that the $F1_2$-CNC had a better viscoelastic response, probably improving the PUF toughness.

3.7. Thermogravimetric weight loss of the PUFs

The weight residue (WR) as a function of temperature of the PUFs prepared from the formulations $F1_1$, $F1_2$-CNC, $F1_2$, $F1_2$-CNC, F2 and F2-CNC is depicted in Fig. 8.

The main graphic focuses the WR associated to the temperature interval between 300 °C and 800 °C while the inset covered the temperature interval between 25 °C and 300 °C. The variation of the WR as a function of temperature is associated to the thermal decomposition of the microstructure of the PUF. The most signifi-

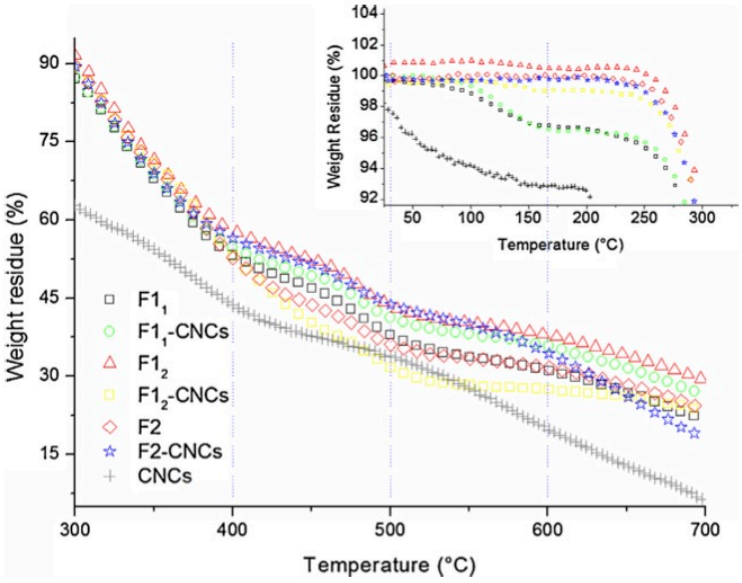

Fig. 8. Weight residue (WR) as a function of temperature of the PUFs and the CNC reinforced PUFs.

cant thermal degradation stages were the HS and SS decomposition, which covered the ranges of temperature located at approximately 300–500 °C and 500–600 °C, respectively (Javni et al., 2000). On the other hand, the WR of the CNC used in this work is also depicted in Fig. 8. The thermal degradation of the CNC covered a wide range of temperature from around 200 °C up to 800 °C. According to what has already been found in literature (Morán et al., 2008; Yang, Yan, Chen, Lee, &, Zheng, 2007), the thermal degradation stages can be associated to the thermal degradation of cellulose, hemicellulose and lignin. Due to the fact that the CNC used in this work had a relevant degradation stage centered at 400 °C, it can be assumed that it was mostly composed of cellulose precursor. These results are in agreement with has already been found in literature (Morán et al., 2008; Yang et al., 2007). An additional aspect which is a key issue to the subsequent discussion is that the CNC were added only to a 0.5 wt.% to the PUF formulation.

By evaluating the WR at a fixed temperature, the thermal resistance of each PUF can be evaluated. Specifically, due to the fact that the thermal degradation stages of the SS and the HS are separated by approximately 100 °C, it can also be distinguished if the thermal resistance of either the SS or the HS were modified. For example, at a temperature fixed at 450 °C, the thermal resistance of the PUFs can be ordered from the highest to the lowest value like this: $F1_2 \approx F2 > F1_1$-CNC > $F1_1$ > F2-CNC > $F1_2$-CNC. In that temperature interval, the main degradation mechanism was associated to the thermal decomposition of the HS, then, it can be assumed that the thermal resistance of the HS of each PUF can be ordered in the same way. This comparison is useful to determine the effect of changing the NCO number, the FI and the CNC content on the thermal degradation resistance of the HS. Then, the increase of the NCO number had the effect of increasing the thermal resistance of the PU, due to a higher WR. This result was expected because a higher NCO number meant a higher HS specific content. Also, the increase of the FI had an identical effect, due to the same reason. In contrast, the addition of CNC in the formulation had different effects. For the case of the PUF prepared with $F1_1$, the incorporation of CNC caused an increase of the thermal resistance of the HS. This is a clear indication that for this particular formulation, the CNC migrated to the HS. This hypothesis can be inferred from the fact that the CNC had a higher relative thermal resistance in that temperature interval (Fig. 8). In contrast, for the case of the PUF prepared with $F1_2$ and F2, the incorporation of CNC in the formulation caused a decrease of the thermal resistance of the HS, an opposite effect with respect to its $F1_1$ counterpart.

An identical analysis can be performed with the region associated to the thermal degradation of the SS (temperature range between 500 and 600 °C). Then, it can be assumed that an increase of FI caused an increase of the thermal resistance of the SS while an increase of the NCO number caused a reduction of the SS thermal resistance. In addition, the incorporation of CNCs in the formulation only caused a substantial increase of the thermal resistance of the SS for the PUFs prepared with F2. For the other formulations ($F1_1$ and $F1_2$), no significant changes were measured. This experimental result is a clear indication that the CNC, for the particular case of the PUF prepared with F2, probably migrated to the SS instead of the HS.

4. Conclusions

PUFs were successfully prepared with varying FI, NCO number and a fixed CNC content (0.5 wt.%). A key aspect for the change of the microstructure of the PUF was associated to the migration of the CNC to either the HS or the SS. For the case of formulation $F1_1$ (lower NCO number and FI), several experimental techniques (DSC, TGA) corroborated that the CNC migrated to the HS, because of the formation of a less compact hydrogen bonded HS region, which indicated that the isocyanate group reacted with the AGU as well as the polyol. In this case the CNC behaved as a HS, improving substantially the mechanical properties (E_c and σ_c improved by 63% and 50%, respectively) of the PUFs. On the other hand, an increase of either the NCO number or the Formulation Index (FI) prevented the migration of the CNC into the HS. This indicated that the CNC behaved as a SS, with weakened or unaltered mechanical properties. It was assumed that substantial hydrogen bonding in-between the SS prevented the migration of the CNC to the HS.

During foam synthesis, the CNC behaved both as a nucleation agent and as a particulate surfactant. For the case of a formulation with low FI and NCO number, the CNC mainly behaved as

a retardant of the cell walls drainage rate, producing a coarser microstructure with thickened struts. On the other formulations, the CNC behaved both as a nucleation agent and a particulate surfactant. The dispersion of the CNC in the PUF matrix was evaluated by means of EDS mapping, a technique which was able to resolve the distribution and agglomeration of the CNC particles in the cell walls and struts. Finally, it was found that the sole measurement of apparent density could lead to non substantiated conclusion about the role of CNC as a nucleation agent. The combination of apparent density measurements and cell size dimensions should be combined to better understand the role of CNC as a nucleation agent.

The results of this research will aid in the development of innovative rigid PUFs formulations with enhanced mechanical properties and a higher content of renewable precursors. This can be obtained through the replacement of the isocyanate precursor with CNC, when the CNC behaved as a HS or by the replacement of the polyol, when it behaved as the SS.

Acknowledgements

The authors would like to thank Dra. Analía Vazquez for its financial support to the research that has been made in this work. Also Matías Nonna (Huntsman), Inés Bergamini (Resikem) and Rafael Goldman (Mentvil) for supplying the reactants.

References

Alvarez, V., & Vázquez, A. (2004). Thermal degradation of cellulose derivatives/starch blends and sisal fibre biocomposites. *Polymer Degradation and Stability*, *84*(1), 13–21.

Aranguren, M. I., Marcovich, N. E., Salgueiro, W., Somoza, A., et al. (2013). Effect of the nano-cellulose content on the properties of reinforced polyurethanes. A study using mechanical tests and positron anihilation spectroscopy. *Polymer Testing*, *32*(1), 115–122.

Aranguren, M. I., Rácz, I., & Marcovich, N. E. (2007). Microfoams based on castor oil polyurethanes and vegetable fibers. *Journal of Applied Polymer Science*, *105*(5), 2791–2800.

Auad, M. L., Contos, V. S., Nutt, S., Aranguren, M. I., & Marcovich, N. E. (2008). Characterization of nanocellulose-reinforced shape memory polyurethanes. *Polymer International*, *57*(4), 651–659.

Besse, V., Auvergne, R., Carlotti, S., Boutevin, G., Otazaghine, B., Caillol, S., et al. (2013). Synthesis of isosorbide based polyurethanes: an isocyanate free method. *Reactive and Functional Polymers*, *73*(3), 588–594.

Brinchi, L., Cotana, F., Fortunati, E., & Kenny, J. M. (2013). Production of nanocrystalline cellulose from lignocellulosic biomass: technology and applications. *Carbohydrate Polymers*, *94*(1), 154–169.

Casado, U., Marcovich, N. E., Aranguren, M. I., & Mosiewicki, M. A. (2009). High-strength composites based on tung oil polyurethane and wood flour: effect of the filler concentration on the mechanical properties. *Polymer Engineering & Science*, *49*(4), 713–721.

Çaylı, G., & Küsefoğlu, S. (2008). Biobased polyisocyanates from plant oil triglycerides: synthesis, polymerization, and characterization. *Journal of Applied Polymer Science*, *109*(5), 2948–2955.

Corcuera, M. A., Rueda, L., Fernandez d'Arlas, B., Arbelaiz, A., Marieta, C., Mondragon, I., et al. (2010). Microstructure and properties of polyurethanes derived from castor oil. *Polymer Degradation and Stability*, *95*(11), 2175–2184.

Cranston, E. D., & Gray, D. G. (2006). Morphological and optical characterization of polyelectrolyte multilayers incorporating nanocrystalline cellulose. *Biomacromolecules*, *7*(9), 2522–2530.

Chen, S., Wang, Q., & Wang, T. (2011). Damping, thermal, and mechanical properties of montmorillonite modified castor oil-based polyurethane/epoxy graft IPN composites. *Materials Chemistry and Physics*, *130*(1–2), 680–684.

Chiacchiarelli, L. M., Monsalve, L., Vázquez, A., Kenny, J. M., & Torre, L. (2014). A polycaprolactone-based compatibilization treatment to improve dispersion and interphase structure of silica polyurethane composites. *Polymer Engineering & Science*, *54*(8), 1817–1826.

Chiacchiarelli, L. M., Escobar, M. M., Kenny, J. M., & Torre, A. (2015). The role of the interphase on the shear induced failure of multiwall carbon nanotubes reinforced epoxy nanocomposites. *Journal of Applied Polymer Science*, *132*(4).

Faruk, O., Sain, M., Farnood, R., Pan, Y., & Xiao, H. (2014). Development of lignin and nanocellulose enhanced bio PU foams for automotive parts. *Journal of Polymers and the Environment*, *22*(3), 279–288.

Fortunati, E., Armentano, I., Zhou, Q., Iannoni, A., Saino, E., Visai, L., et al. (2015). Multifunctional bionanocomposite films of poly(lactic acid), cellulose nanocrystals and silver nanoparticles. *Carbohydrate Polymers*, *87*(2), 1596–1605.

Fortunati, E., Armentano, I., Zhou, Q., Puglia, D., Terenzi, A., Berglun, L. A., et al. (2012). Microstructure and nonisothermal cold crystallization of PLA composites based on silver nanoparticles and nanocrystalline cellulose. *Polymer Degradation and Stability*, *97*(10), 2027–2036.

Hojabri, L., Kong, X., & Narine, S. S. (2009). Fatty acid-derived diisocyanate and biobased polyurethane produced from vegetable oil: synthesis, polymerization, and characterization. *Biomacromolecules*, *10*(4), 884–891.

Javni, I., Petrovic, Z. S., Guo, A., & Fuller, R. (2000). Thermal stability of polyurethanes based on vegetable oils. *Journal of Applied Polymer Science*, *778*, 1723–1734.

Juntaro, J., Ummartyotin, S., Sain, M., & Manuspiy, H. (2012). Bacterial cellulose reinforced polyurethane-based resin nanocomposite: a study of how ethanol and processing pressure affect physical, mechanical and dielectric properties. *Carbohydrate Polymers*, *87*(4), 2464–2469.

Klemm, D., Heublein, B., Fink, H. P., & Bohn, A. (2005). Cellulose: fascinating biopolymer and sustainable raw material. *Angewandte Chemie International Edition*, *44*(22), 3358–3393.

Klemm, D., Schmauder, H. P., & Heinze, T. (2005). Cellulose. *Biopolymers Online*.

Lee, H. S., Wang, Y. K., & Hsu, S. L. (1987). Spectroscopic analysis of phase separation behavior of model polyurethanes. *Macromolecules*, *20*(9), 2089–2095.

Li, Y., & Ragauskas, A. J. (2011). Cellulose nano whiskers as a reinforcing filler in polyurethanes. *Algae*, *75*(80), 10–15.

Li, Y., & Ragauskas, A. J. (2012). Ethanol organosolv lignin-based rigid polyurethane foam reinforced with cellulose nanowhiskers. *RSC Advances*, *2*(8), 3347–3351.

Li, Y., Ren, H., & Ragauskas, A. J. (2010). Rigid polyurethane foam reinforced with cellulose whiskers: synthesis and characterization. *Nano-Micro Letters*, *2*(2), 89–94.

Li, Y., Ren, H., & Ragauskas, A. J. (2011). Rigid polyurethane foam/cellulose whisker nanocomposites: preparation, characterization, and properties. *Journal of Nanoscience and Nanotechnology*, *11*(8), 6904–6911.

Lin, S., Huang, J., Chang, P. R., Wei, S., Xu, Y., & Zhang, Q. (2013). Structure and mechanical properties of new biomass-based nanocomposite: castor oil-based polyurethane reinforced with acetylated cellulose nanocrystal. *Carbohydrate Polymers*, *95*(1), 91–99.

Modesti, M., & Lorenzetti, A. (2001). An experimental method for evaluating isocyanate conversion and trimer formation in polyisocyanate–polyurethane foams. *European Polymer Journal*, *37*(5), 949–954.

Morán, J. I., Alvarez, V. A., Cyras, V. P., Vázquez, A., et al. (2008). Extraction of cellulose and preparation of nanocellulose from sisal fibers. *Cellulose*, *15*(1), 149–159.

Mosiewicki, M. A., Casado, U., Marcovich, N. E., & Aranguren, M. I. (2009). Polyurethanes from tung oil: polymer characterization and composites. *Polymer Engineering & Science*, *49*(4), 685–692.

Mosiewicki, M. A., Dell'Arciprete, G. A., Aranguren, M. I., & Marcovich, N. E. (2009). Polyurethane foams obtained from castor oil-based polyol and filled with wood flour. *Journal of Composite Materials*, *43*(25), 3057–3072.

Mosiewicki, M. A., Rojek, P., Michałowski, S., Aranguren, M. I., & Prociak, A. (2015). Rapeseed oil-based polyurethane foams modified with glycerol and cellulose micro/nanocrystals. *Journal of Applied Polymer Science*, *132*(10).

Özgür Seydibeyoğlu, M., & Oksman, K. (2008). Novel nanocomposites based on polyurethane and micro fibrillated cellulose. *Composites Science and Technology*, *68*(3–4), 908–914.

Petrovič, Z. S., Cho, Y. J., Javni, I., Magonov, S., Yerina, N., Schaefer, D. W., et al. (2004). Effect of silica nanoparticles on morphology of segmented polyurethanes. *Polymer*, *45*(12), 4285–4295.

Randall, D., & Lee, S. (2003). *The polyurethanes book*. Wiley.

Rivera-Armenta, J. L., Heinze, T., & Mendoza-Martínez, A. M. (2004). New polyurethane foams modified with cellulose derivatives. *European Polymer Journal*, *40*(12), 2803–2812.

Rueda, L., Saralegui, A., Fernández d'Arlas, B., Zhou, Q., Berglund, L. A., Corcuera, M. A., et al. (2013). Cellulose nanocrystals/polyurethane nanocomposites. Study from the viewpoint of microphase separated structure. *Carbohydrate Polymers*, *92*(1), 751–757.

Silva, M. C., Takahashi, J. A., Chaussy, D., Belgacem, M. N., & Silva, G. G. (2010). Composites of rigid polyurethane foam and cellulose fiber residue. *Journal of Applied Polymer Science*, *117*(6), 3665–3672.

Szycher, M. (1999). *Szycher's handbook of polyurethanes*. New York, USA: CRC Press LLC.

Tamami, B., Sohn, S., & Wilkes, G. L. (2004). Incorporation of carbon dioxide into soybean oil and subsequent preparation and studies of nonisocyanate polyurethane networks. *Journal of Applied Polymer Science*, *92*(2), 883–891.

Tien, Y. I., & Wei, K. H. (2001). Hydrogen bonding and mechanical properties in segmented montmorillonite/polyurethane nanocomposites of different hard segment ratios. *Polymer*, *42*(7), 3213–3221.

Wik, V., Aranguren, M., & Mosiewicki, M. (2011). Castor oil-based polyurethanes containing cellulose nanocrystals. *Polymer Engineering & Science*, *51*(7), 1389–1396.

Yang, H., Yan, R., Chen, H., Lee, D. H., & Zheng, C. (2007). Characteristics of hemicellulose, cellulose and lignin pyrolysis. *Fuel*, *86*(12), 1781–1788.